Supporting Information.

Acetylcholinesterase Inhibitors with Photoswitchable Inhibition of β-Amyloid-Aggregation

Xinyu Chen[†,‡], Sarah Wehle[‡], Natascha Kuzmanovic[§], Benjamin Merget[‡], Ulrike Holzgrabe[‡], Burkhard König[§], Christoph A. Sotriffer[‡], Michael Decker[†,‡] *

[†]Institut für Pharmazie, [§]Institut für Organische Chemie, Universität Regensburg, Universitätsstraße 31, 93053 Regensburg, Germany, [‡]Institut für Pharmazie und Lebensmittelchemie, Julius-Maximilians-Universität Würzburg, Am Hubland, 97074 Würzburg, Germany

Table of Contents:

Spectral data of target compounds

10a:

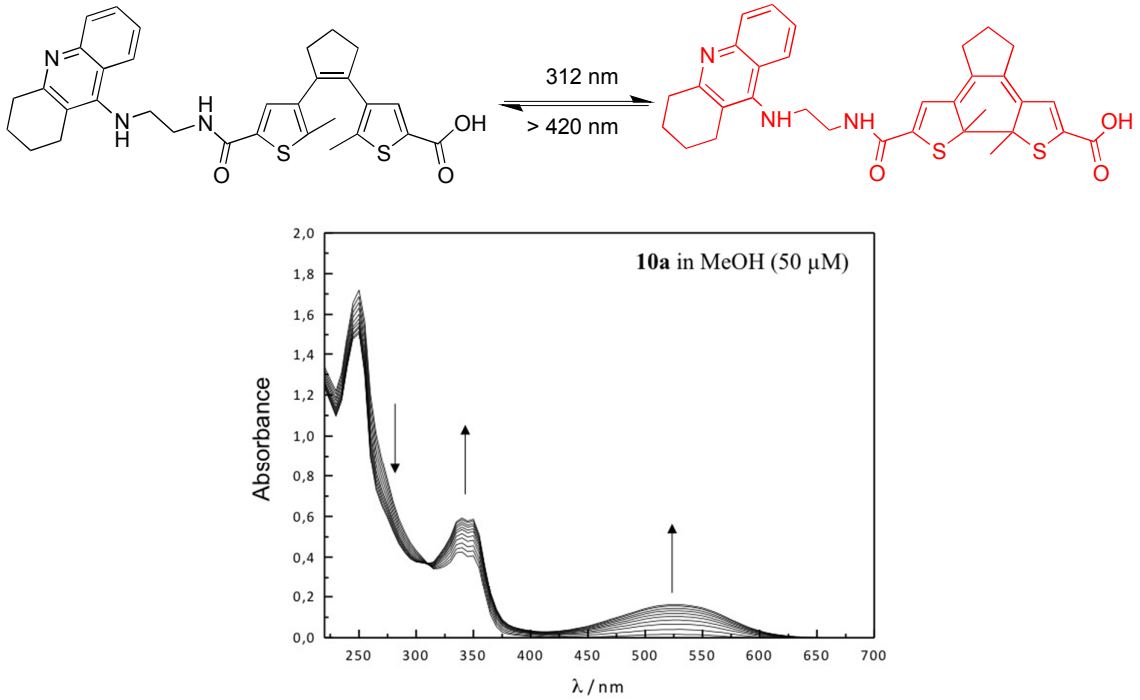

Figure 1. UV-Vis absorption spectra evolution of compound **10a** dissolved in methanol (50 µM) by irradiation with 312 nm light. Arrows indicate the changes of the absorption maxima with irradiation periods of 6 s.

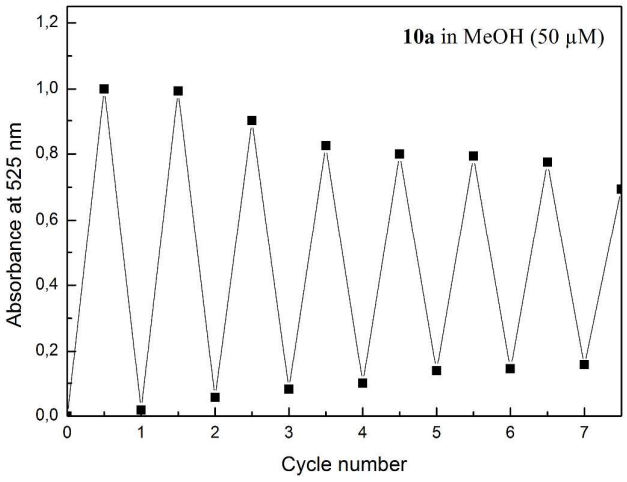

Figure 2. Cycle performance of compound **10a**, changes in absorption at 525 nm during an alternated irradiation of a solution in MeOH (50 µM) with 312 nm light for 60 s and greater than 420 nm light for 15 min.

10b:

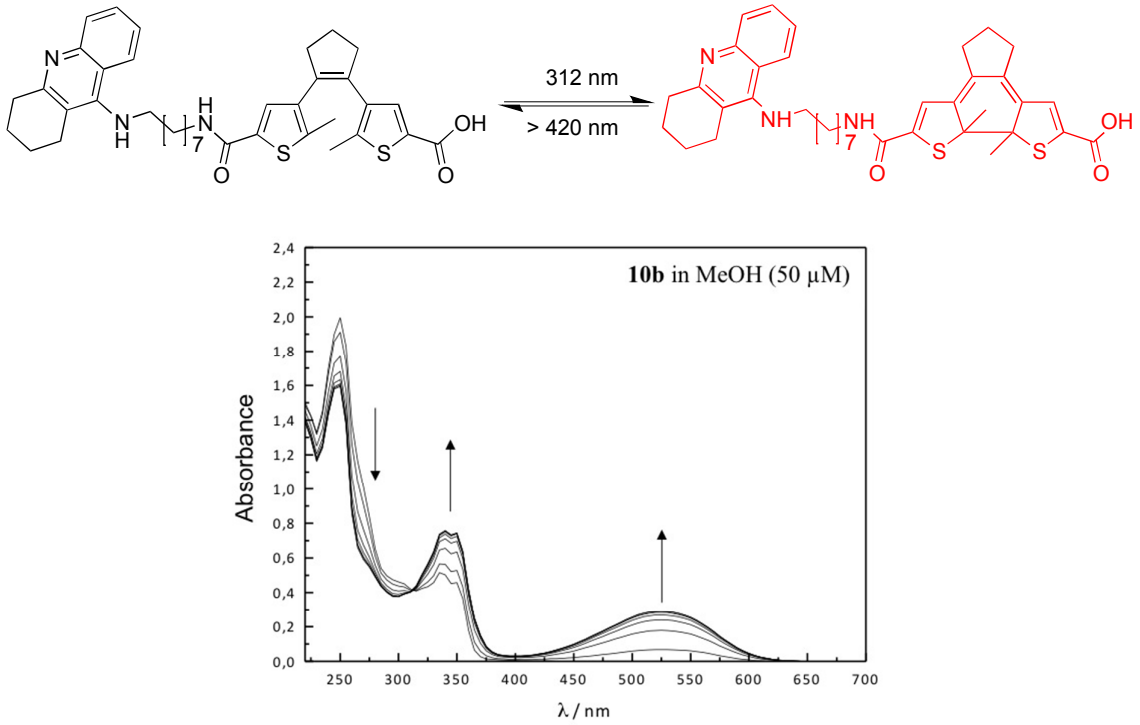

Figure 3. UV-Vis absorption spectra evolution of compound **10b** dissolved in methanol (50 µM) by irradiation with 312 nm light. Arrows indicate the changes of the absorption maxima with irradiation periods of 6 s.

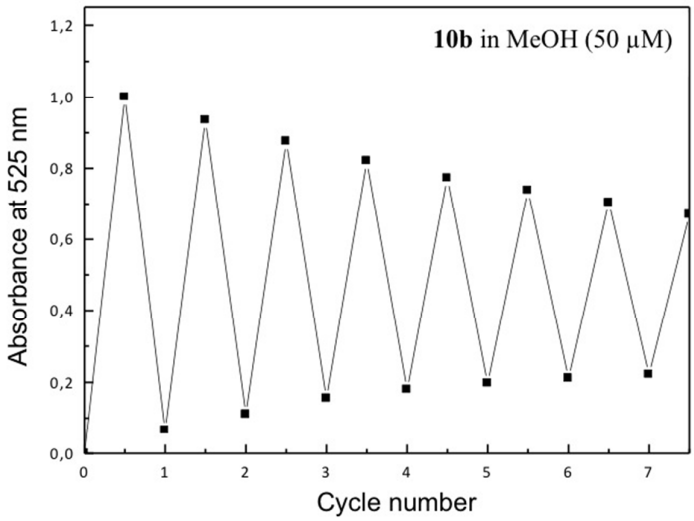

Figure 4. Cycle performance of compound **10b**, changes in absorption at 525 nm during an alternated irradiation of a solution in MeOH (50 µM) with 312 nm light for 60 s and greater than 420 nm light for 15 min.

11a:

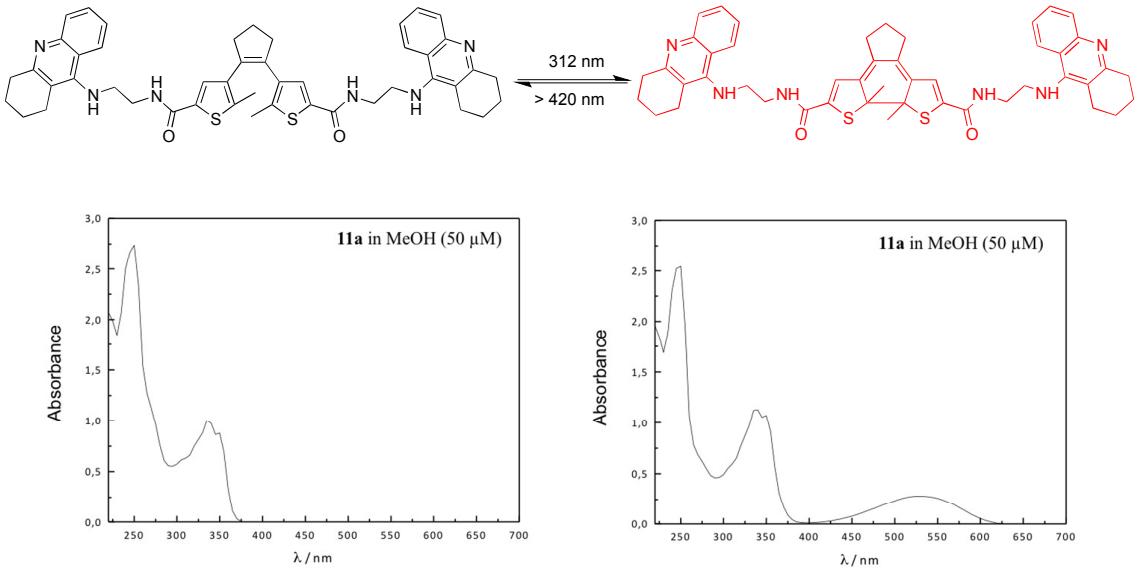

Figure 5. Absorption spectra of **11a** in its ring-opened photoisomer (**11a** open, left) and its ring-closed one (**11a-close**, right).

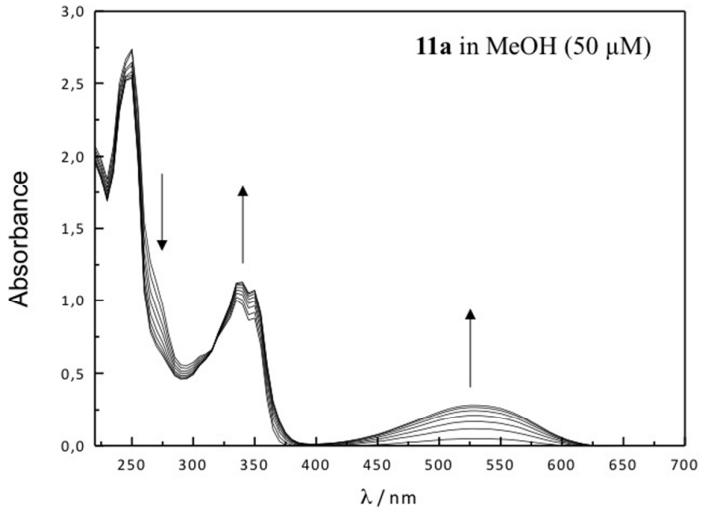

Figure 6. UV-Vis absorption spectra evolution of compound **11a** dissolved in methanol (50 µM) by irradiation with 312 nm light. Arrows indicate the changes of the absorption maxima with irradiation periods of 6 s.

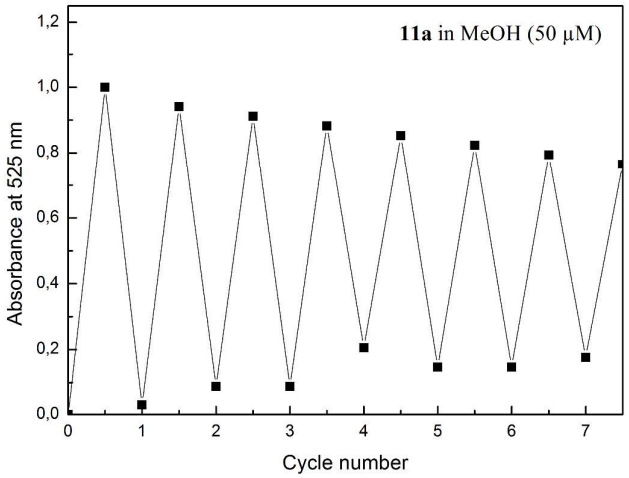

Figure 7. Cycle performance of compound **11a**, changes in absorption at 260 nm (black) and 540 nm (blue) during an alternated irradiation of a solution in methanol (50 μM) with 312 nm light for 60 s and greater than 420 nm light for 15 min.

The photostationary state of the ring-closed photoisomer in a methanol solution (50 μM) was reached after 30 s of irradiation with 312 nm light as shown in the HPLC-chromatograms in Error! Reference source not found.**8** and **9**. We performed the studies exemplarily with compound **11b** by analytical HPLC-MS detecting absorption at 525 nm.

Since all samples for the ChEs inhibition assay were used in concentrations lower than 50 μM, the conversion to the ring-closed photoisomers was assumed to be quantitative after 15 min of UV irradiation and the results achieved for the ring-closed photoisomers were reliable and totally dependent on the activities of the ring-closed form.

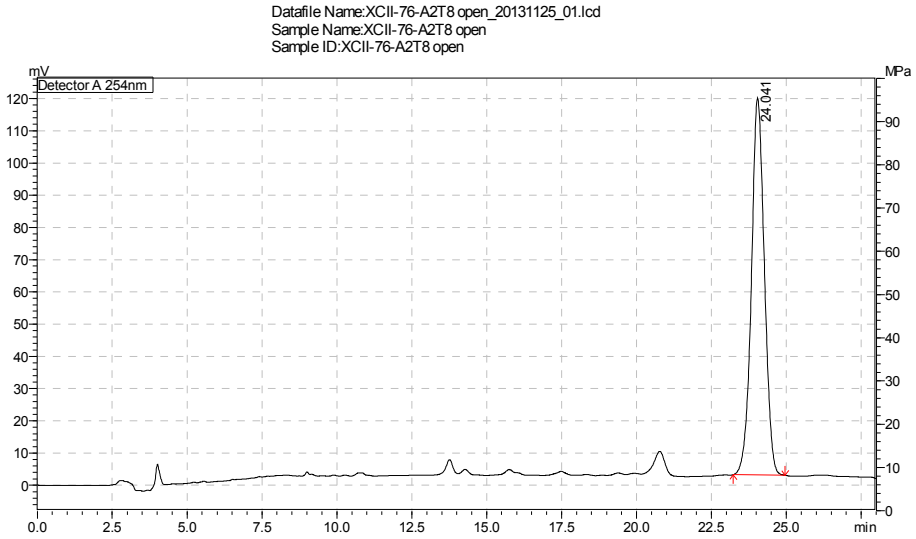

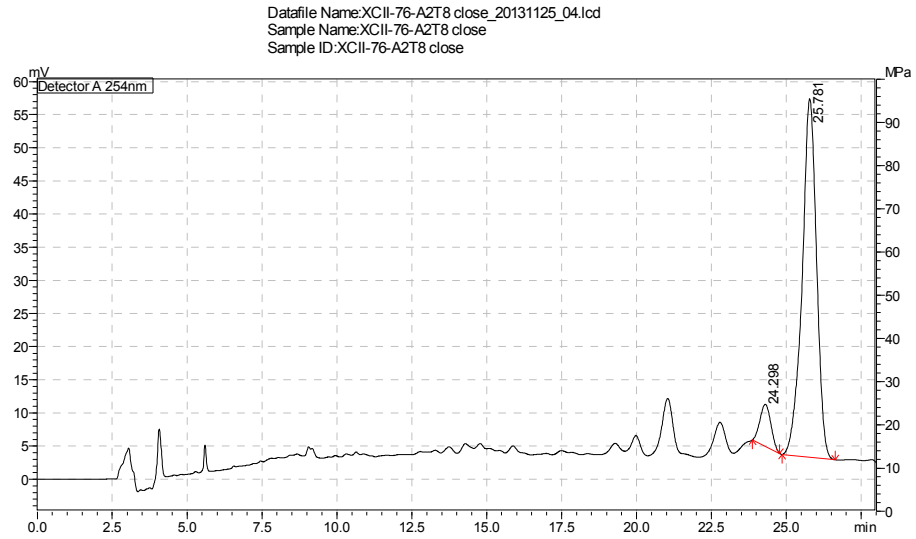

Figure 8. The HPLC chromatography of both ring-opened (above) and ring-closed (below) forms (10 μM in buffer solution, pH = 8.0).

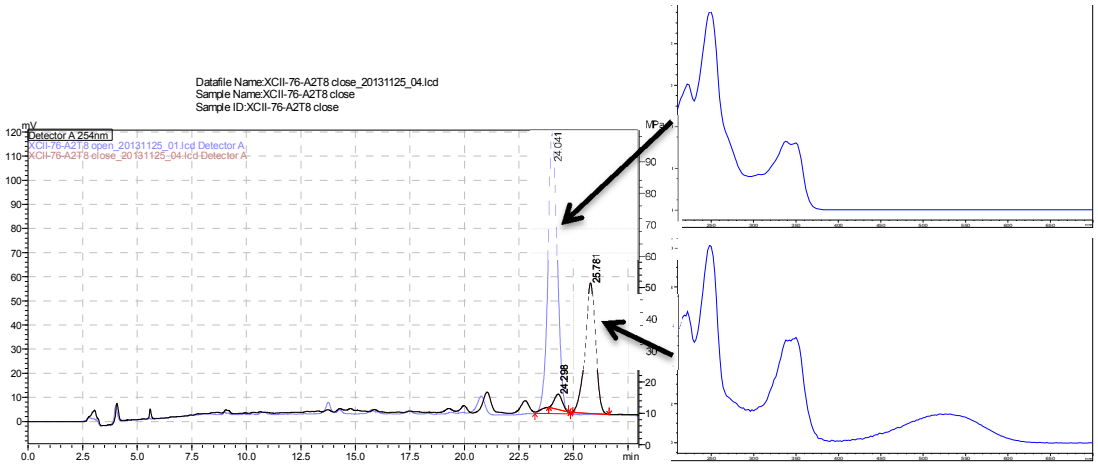

Figure 9. Overlap of chromatograms of both photochromic forms on HPLC (100 μM in buffer solution, pH = 8.0): Ring-opened (blue line) and -closed (dark red) forms with respective UV-Vis absorbance. The chromatogram of ring-closed form was irradiated for 30 s indicate that 92% of the open isomer was converted to the closed one (absorption at 525 nm). HPLC: Shimadzu, 150*4.6 mm Phenomenex C18 column, A) Millipore water + 0.1% TFA, B) Acetonitrile + 0.2% TFA, 1mL/min flow rate, from 30% to 55% for 5 min, remain 20 min and drop to 30% in 3 min.

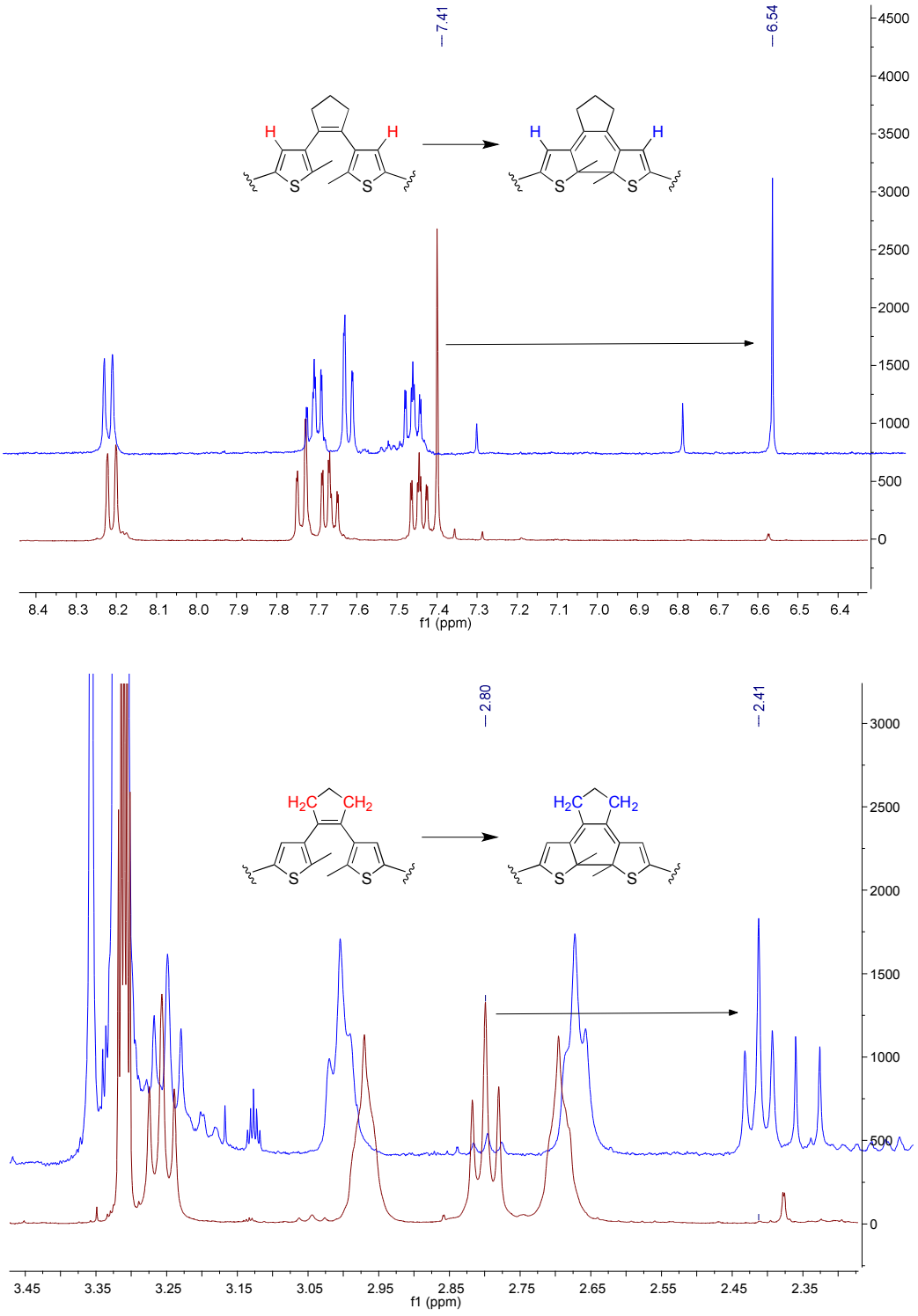

Figure 10. The chemical shift changing from ring-opened form (red) to ring-closed form (blue) at both aromatic area (above) and aliphatic area (below).

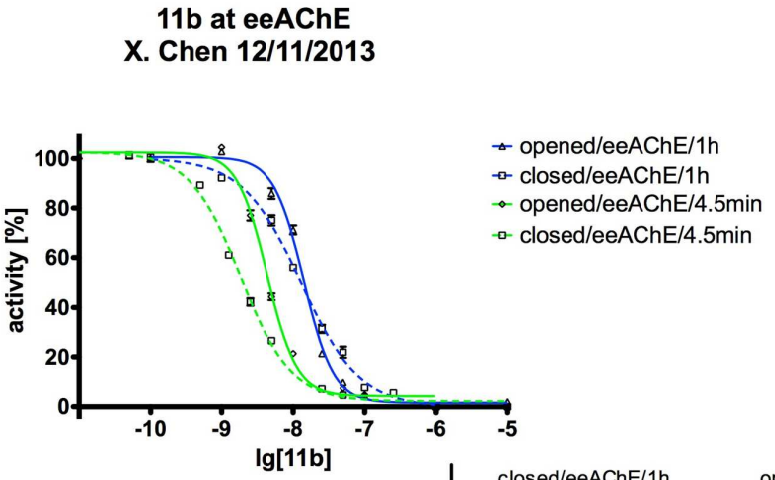

	closed/eeAChE/1h	opened/eeAChE/1h	opened/eeAChE/4.5min	closed/eeAChE/4.5min
Sigmoidal dose-response (variable slope)				
Best-fit values				
Bottom	-0.2672	1.555	4.283	2.179
Top	100.2	100.6	102.5	102.6
LogEC50	-7.889	-7.854	-8.365	-8.735
HillSlope	-1.057	-2.077	-2.087	-1.225
EC50	1.291e-008	1.400e-008	4.317e-009	1.842e-009
Std. Error				
Bottom	1.485	1.129	1.250	1.094
Top	1.511	1.254	1.373	1.189
LogEC50	0.02555	0.01621	0.01701	0.01939
HillSlope	0.06228	0.1233	0.1535	0.06626
95% Confidence Intervals				
Bottom	-3.340 to 2.805	-0.7859 to 3.896	1.697 to 6.870	-0.08528 to 4.444
Top	97.11 to 103.4	97.99 to 103.2	99.62 to 105.3	100.2 to 105.1
LogEC50	-7.942 to -7.836	-7.887 to -7.820	-8.400 to -8.330	-8.775 to -8.695
HillSlope	-1.185 to -0.9278	-2.333 to -1.822	-2.405 to -1.770	-1.363 to -1.088
EC50	1.143e-008 to 1.458e-008	1.296e-008 to 1.513e-008	3.981e-009 to 4.682e-009	1.679e-009 to 2.020e-009
Goodness of Fit				
Degrees of Freedom	23	22	23	23
R square	0.9949	0.9954	0.9935	0.9958
Absolute Sum of Squares	185.2	212.5	312.3	174.9
Sy.x	2.838	3.108	3.685	2.758
Number of points				
Analyzed	27	26	27	27

11b at hAChE
X. Chen 12/11/2013

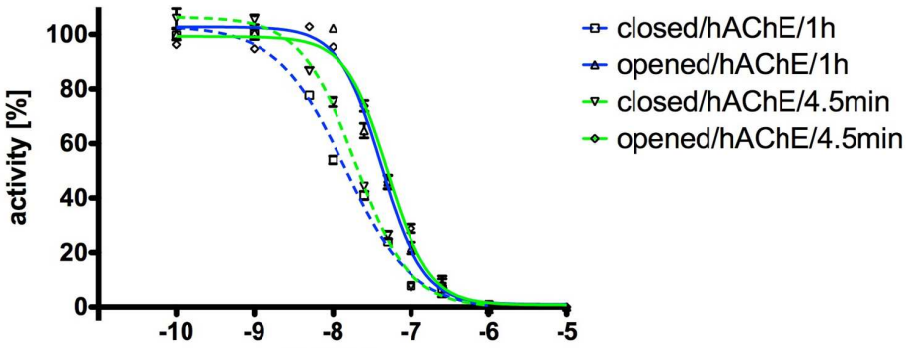

	closed/hAChE/1h	opened/hAChE/1h	closed/hAChE/4.5min	opened/hAChE/4.5min
Sigmoidal dose-response (variable slope)				
Best-fit values				
Bottom	-0.8405	0.9872	-0.1054	0.7888
Top	103.2	102.8	106.4	99.26
LogEC50	-7.849	-7.383	-7.718	-7.305
HillSlope	-1.001	-1.603	-1.242	-1.617
EC50	1.417e-008	4.142e-008	1.914e-008	4.956e-008
Std. Error				
Bottom	2.324	2.046	2.058	1.770
Top	2.238	2.088	1.887	1.481
LogEC50	0.03816	0.02937	0.02992	0.02370
HillSlope	0.08408	0.1568	0.09224	0.1374
95% Confidence Intervals				
Bottom	-5.649 to 3.968	-3.247 to 5.221	-4.363 to 4.152	-2.873 to 4.451
Top	98.53 to 107.8	98.48 to 107.1	102.5 to 110.3	96.20 to 102.3
LogEC50	-7.928 to -7.770	-7.444 to -7.322	-7.780 to -7.656	-7.354 to -7.256
HillSlope	-1.175 to -0.8272	-1.928 to -1.279	-1.432 to -1.051	-1.901 to -1.332
EC50	1.182e-008 to 1.700e-008	3.601e-008 to 4.764e-008	1.660e-008 to 2.207e-008	4.427e-008 to 5.548e-008
Goodness of Fit				
Degrees of Freedom	23	23	23	23
R square	0.9896	0.9864	0.9913	0.9904
Absolute Sum of Squares	390.3	637.9	389.6	405.5
Sy.x	4.119	5.267	4.116	4.199
Number of points				
Analyzed	27	27	27	27

Figure 11. Inhibition curves of **11b** at *ee*AChE and *h*AChE as both ring-opened and -closed forms.

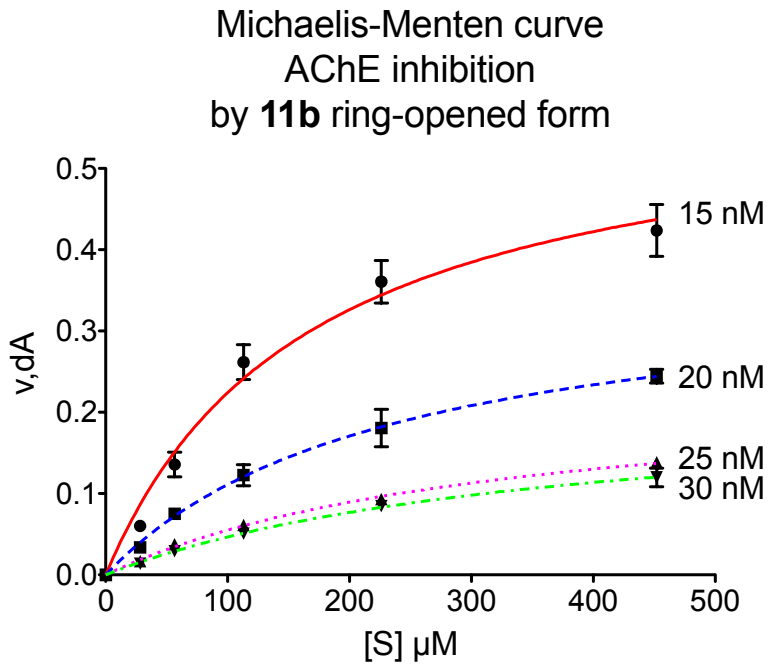

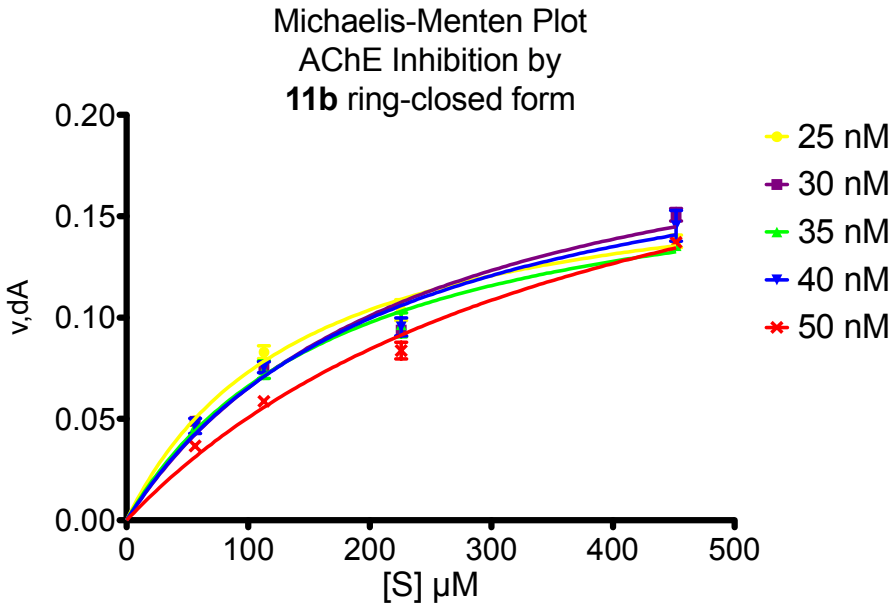

Figure 12. Substrate-velocity curves (Michaelis-Menten) of eeAChE activity with different substrate concentration (28.2-452 µM) in the presence of 15-30 nM compound **11b** in its ring-opened form and 25-50 nM compound **11b** in its ring-closed form.

Supplementary figures of computational modeling

Table 1. Scores of the top five GOLD docking results (obtained with the ASP scoring function) for **11b** closed and **11b** open, as well as DSX rescoring results and reranking of the corresponding five poses.

Rank (GOLD/ASP)	Score (GOLD/ASP)	Rescoring (DSX)	Rescoring rank (DSX)
	11b closed		
1	108.33	−212.65	2
2	**105.79**	**−241.23**	**1**
3	96.98	−203.07	4
4	96.90	−210.06	3
5	94.97	−197.75	5
	11b open		
1	114.20	−238.62	2
2	**106.91**	**−253.19**	**1**
3	100.23	−209.64	3
4	98.80	−205.64	4
5	98.74	−199.97	5

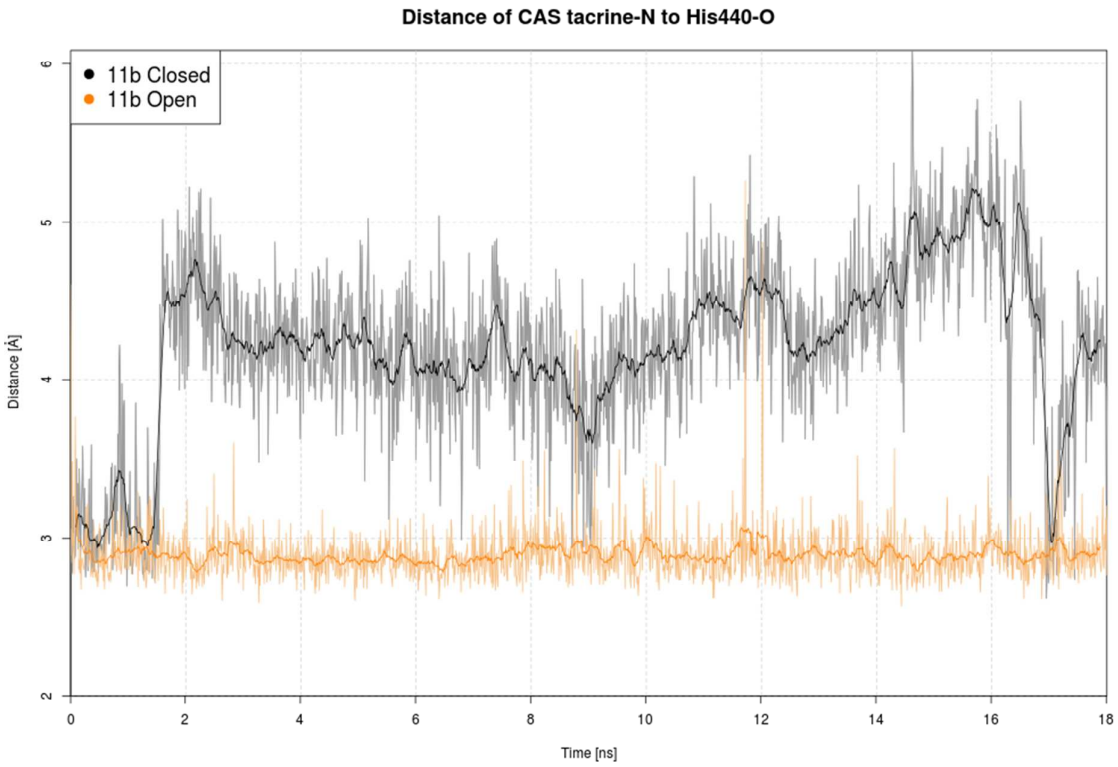

Figure 13. Distance of the tacrine aromatic nitrogen in the CAS to the His440 carbonyl oxygen of **11b** open and **11b** closed along the MD trajectories of 18 ns. Light colors depict the RMSD curve measured at each frame (10 ps), dark colors represent a moving average with a window size of 20 frames.